Logarithmic correction of the electric susceptibility in paraelectric tris-sarcosine calcium chloride

Erik Sandvold* and Eric Courtens
IBM Zurich Research Laboratory, CH-8803 Rüschlikon, Switzerland
(Received 9 September 1982; revised manuscript received 24 January 1983)

The dielectric constant tris-sarcosine calcium chloride [$(CH_3\text{-}NH\text{-}CH_2\text{-}COOH)_3\cdot CaCl_2$] has been measured with a relative precision of ~ 0.0005 from the transition temperature T_c to T_c+60 K. Over more than 2 orders of magnitude of reduced temperature $[(T-T_c)/T_c]$, it follows accurately the logarithmically corrected mean-field behavior of uniaxial dipolar ferroelectrics. It is shown unambiguously that these corrections are superior to a power law. Close to T_c ($T<T_c+0.3$ K), the dielectric constant becomes affected by roundoff effects. Previous results on tris-sarcosine calcium chloride are reviewed in the light of these new findings.

I. INTRODUCTION

Tris-sarcosine calcium chloride (TSCC), a molecular salt of formula $(CH_3\text{-}NH\text{-}CH_2\text{-}COOH)_3\cdot CaCl_2$, exhibits a uniaxial paraelectric-to-ferroelectric transition on cooling below $T_c \simeq 130$ K.[1] Early measurements of its dielectric and thermal properties were performed mainly by Makita.[2] The structure of the paraelectric phase is orthorhombic, with space-group $Pnma$,[3] whereas the ferroelectric phase is believed to have space-group $Pn2_1a$. The latter is derived from the former by suppression of the planes of reflection symmetry perpendicular to the ferroelectric b axis. All sarcosine molecules are found to be in the zwitter-ion configuration $CH_3\text{-}NH_2^+\text{-}CH_2\text{-}COO^-$, whereas the protons form very asymmetric hydrogen bonds N—H $\cdots$ Cl, with an N-H distance typically equal to one-half the H $\cdots$ Cl distance.[3] For this reason, it can be expected that dipolar interactions between the strongly polar sarcosines play an important role in the transition, making TSCC an *a priori* much better candidate than triglycine sulfate (TGS)[4,5] for the observation of uniaxial dipolar behavior in a paraelectric.[6]

There has been a considerable amount of recent work on the dielectric properties of TSCC and on its partially brominated isomorphs TSCCB. The measurements on the paraelectric phase have usually been explained using various variants of Landau theory,[7–12] leading to an unusual spread of values for the Curie constant.[13] This difficulty might not be surprising in view of the exceptional relative importance of the dielectric background far away from T_c, and of roundoff effects close to T_c, both influences having received insufficient attention in some of the previous works. However, this spread might also be indicative of a Curie-Weiss law being only an approximation to the true critical behavior, making the effective Curie constant strongly dependent on the temperature range from which it is derived. Related difficulties have been noted in comparisons of low-temperature dielectric,[7,8,11] electro-optic,[14] and EPR measurements,[15,16] from which temperature-dependent polarization exponents β_{eff} have been derived.

Furthermore, there is a current debate as to the nature of the transition mechanism, be it order-disorder or displacive. Although there is some evidence for the former case,[2,17,18] a soft TO mode has been observed in the ferroelectric phase.[19–24] The most recent publications[23,24] indicate that its squared frequency ω_{TO}^2 varies considerably from liquid He to T_c-2 K, establishing a definite displacive character to the transition. However, the small LO-TO splitting[19,20] has been taken as a counterargument,[21] and the possibilities of either two successive transitions,[22] or of a cell-doubling transition,[19] have been raised. On the other hand, a careful calorimeter study has demonstrated rather clearly the existence of a single thermal anomaly.[25] That data has recently been interpreted in terms of logarithmic corrections that could be fitted over narrow temperature ranges on both sides of the transition.[26]

Under these conditions, it appeared worthwhile performing an accurate measurement of the paraelectric susceptibility and comparing it with the predictions of the Larkin-Khmelnitzkii (LK) theory for uniaxial ferroelectrics.[27] This is all the more so, as the only other known experimental example of logarithmic corrections in ferroelectrics is for trigly-

cine sulfate (TGS).[5] In that case, there can be profound effects of crystal imperfections, as crystals are most often grown at temperatures below T_c and are then much less perfect, as recently demonstrated by Strukov *et al.*[28] Logarithmic corrections have, of course, been demonstrated in other systems, the best example being the uniaxial ferromagnet $LiTbF_4$.[29] This paper presents measurements of ϵ_b, the dielectric constant in the direction parallel to the ferroelectric axis of TSCC, in the range T_c to T_c+120 K. Given our relative accuracy of ~ 0.0005, we have been able to detect the contribution of logarithmic corrections over the temperature range $T_c+0.3$ K to T_c+60 K. Closer to T_c the results are affected by roundoff. Section II presents the experimental details, in particular the care taken in sample preparation and annealing. Section III explains the various fits performed on the data, and demonstrates that logarithmic corrections produce a superior agreement between theory and experiment. Section IV discusses some other literature data in view of the present results. In particular, it shows that the small LO-TO splitting observed is not in disagreement with the Lyddane-Sachs-Teller (LST) relation.

II. EXPERIMENTAL

The sample used in the present measurement was cut from a crystal grown from a seed suspended in a TSCC aqueous solution.[30] The crystal had the shape of a distorted hexagonal prism of height ~ 10 mm. Observations between crossed polarizers revealed that it was twinned, although not as badly as in the case of crystals grown from unseeded solutions (see Ref. 31, Fig. 1). The sample was cut from a large untwinned face, and its final dimensions after polishing were $7.3\times 5.5\times 1.6$ mm^3, with the a axis parallel to the largest dimension and the b axis perpendicular to the largest face. Gold electrodes were sputtered on both large faces, and traces of gold were carefully removed from the side faces. Copper wires of 50 μm diam were attached to these electrodes with a drop of silver paint. For the final data, the only one presented in detail here, these copper wires were replaced by brass wires of the same diameter, thus reducing the thermal disturbance as discussed in the next section.

A first measurement on this sample gave a peak dielectric constant $\epsilon_{b,\max}\simeq 400$. The sample was then annealed in an attempt to reduce the defect density.[32] Since the high-temperature phase is ferroelastic,[31] a uniaxial compressive stress of about 10 N/cm^2 was applied along b during annealing. It is expected that this stress helps to maintain the b direction.[31] The stress jig consisted of two parallel plates pressed together by a spring. Gold foils were placed between sample and plates to improve pressure homogeneity. The jig was bathed in water-free pentadecane in a closed container and held at 140 °C for 20 hours. This led to $\epsilon_{b,\max}\simeq 800$. Repeating the annealing, this time at 150 °C for 100 h, the final value $\epsilon_{b,\max}\simeq 1000$ was obtained.

The dielectric measurements were carried out in equipment originally designed for the detection of flexure resonances.[33] To this effect, the sample is mounted in a strain-free manner, simply hanging from its own wires. The capacitance C and parallel conductance G are measured with a General Radio model-1621 precision capacitance measurement system. The rms field applied to the sample was 2 V/cm at a frequency of 1 kHz. Under these conditions, the capacitance can be measured with a precision of ~ 0.5 to 1 fF, giving a relative precision slightly better than 10^{-3} for our smallest capacitance value ~ 1 pF.

The temperature in the cryostat was regulated using a Pt-resistance sensor in a dc bridge. A separate Pt resistance, with an ac bridge consisting of a resistance standard, a Dekatran DT72A seven-decade transformer, and a lock-in detector were used for thermometry. This provided for a 0.1-mK resolution in temperature reading. With He exchange gas in the cryostat, a stability of 0.5 to 1 mK could be achieved, meaning that our measurement precision became limited by the temperature stabilization at about 1 K above T_c. It was also checked that the measurements were reproducible to 1 mK. The Pt thermometer was specified to follow closely the DIN Standard 43760, with deviations smaller than 30% of those allowed by the norm. The bridge ratios were converted to temperature using a fourth-degree polynomial fit to the DIN curve.[34] Although the relative T measurements are rather precise, the absolute T accuracy can only be claimed to ~ 0.5 K. Furthermore, the great advantage of strain-free sample mounting has the accompanying disadvantage of relatively poor thermal contact with the regulated surroundings and with the thermometer. In particular, the leads from which the sample is hanging can produce temperature inhomogeneities to which we shall revert in the next section.

A good approximation for the dielectric constant ϵ_b is obtained using

$$C=\frac{\epsilon_0\epsilon_b S}{d}\ , \tag{1}$$

where S is the sample area, d its thickness, and ϵ_0 the dielectric constant of vacuum. However, in view of the smallness of both ϵ_b and S, fringing-field effects are not totally negligible. An expression for C

taking fringing fields into account is derived in the Appendix, and it was used to extract ϵ_b from our data. It should be remarked that the fringing-field correction did not in any way change the qualitative nature of the fit results presented in the following section, the main effect of the correction being to reduce the noncritical or background part of the dielectric constant. A tabulation of the original data and of ϵ_b is available separately.[35]

III. RESULTS AND FITS

Figure 1 is a logarithmic presentation of the real part of the measured dielectric constant. For the purpose of this plot, the reduced temperature,

$$t=(T-T_c)/T_c \ , \tag{2}$$

was obtained using for T_c the value at the peak of ϵ_b, $T_c=130.785$ K. The background ϵ_{b0} was estimated from the region where the critical contribution is small ($\epsilon_{b0}=3.2$). Figure 2 shows the corresponding loss tangent

$$\tan\delta \equiv G/\omega C \ , \tag{3}$$

where ω is the measuring frequency. This quantity is negligibly small above $T_c+0.6$ K. Closer to T_c, it starts growing with an initial slope $\tilde{\gamma}$ which might be of the order of -1.5, in agreement with defect theories.[36] However, beyond the point x indicated by arrows in Figs. 1 and 2, the growth of the losses becomes faster. Those measurements ($T<T_x$) have not been included in our fits for reasons discussed below. Points above y ($T>T_y$ in Fig. 1), have also been discarded, and this for two reasons: (i) the relative precision becomes worse than 5×10^{-4} for these points, and (ii) the relative contribution of the critical part $(\epsilon_b-\epsilon_{b0})/\epsilon_b$ becomes rather small, so that the exact temperature dependence of the background ϵ_{b0} might start playing a role.

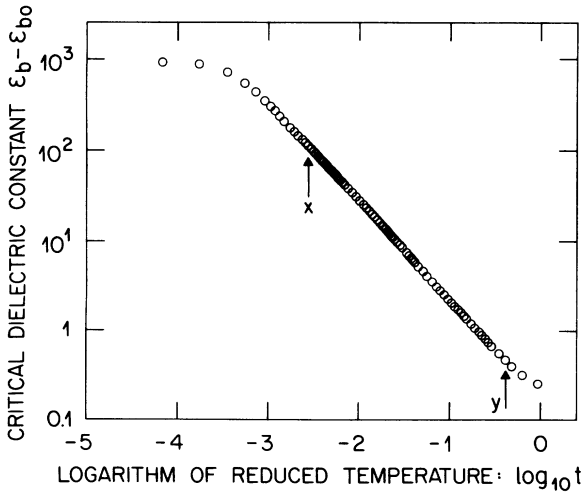

FIG. 1. The real part of the measured dielectric constant parallel to the b axis. The open circles are centered on the measured values, and their size does not indicate the imprecision.

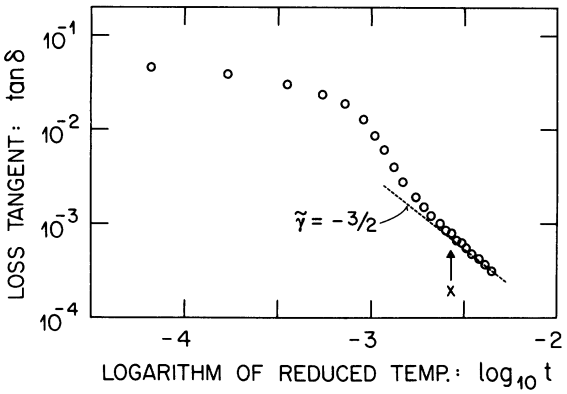

FIG. 2. The loss tangent measured parallel to the b axis. The line $\tilde{\gamma}=-\frac{3}{2}$ is shown as guide to the eye.

The relative precision of the points from y to x is approximately constant, of the order of 5×10^{-4}, as demonstrated by the deviation plot presented below. This is due to the combined effect of the capacitance-measurement precision and the temperature precision. The former is limiting at the high end and the latter at the low end of the range. Hence, it is appropriate to make nonlinear least-

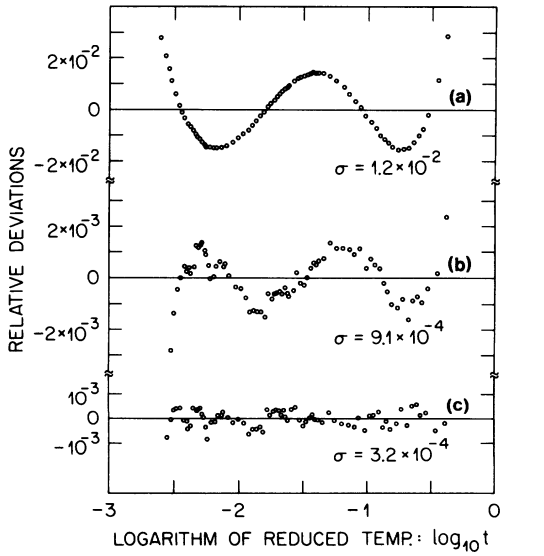

FIG. 3. The relative deviations of the data points from x and y in Fig. 1 fitted to various models. (a) Curie-Weiss with T-dependent background; (b) power law with T-dependent background; (c) log-corrected mean field with constant background. The variance σ of these fits is also indicated.

square fits to the logarithm of the data, $w=\ln\epsilon_b$. The deviations, $\Delta w=\Delta\epsilon_b/\epsilon_b$, are then immediately *relative* deviations, as presented in Fig. 3. The quantities plotted in ordinate in that figure are the calculated minus the measured values. For the fits, we used a nonlinear estimation procedure developed by Marquardt,[37] and available to us as APL (A Programming Language) routines, including significance tests.

As first obvious attempt, the data is fitted to the Curie-Weiss behavior,

$$\epsilon_b=(\epsilon_{b0}+\epsilon_{b1}T)+\frac{M}{t} . \tag{4}$$

The linear temperature dependence of the background (ϵ_{b1}) was added in an effort to improve the fit which then has four parameters: ϵ_{b0}, ϵ_{b1}, M, and T_c. The estimators obtained are

$$\epsilon_{b0}=0.81\pm0.29 , \tag{5a}$$

$$\epsilon_{b1}=0.0125\pm0.0018 , \tag{5b}$$

$$M=0.273\pm0.002 , \tag{5c}$$

$$T_c=130.831\pm0.005 , \tag{5d}$$

where ϵ_{b1} is measured in units of K^{-1} and T_c is measured in units of K. The uncertainty limits indicated are 90% confidence intervals. These are only meaningful, of course, if (4) has the right functional form, which is not the case by far, as indicated by the deviation plot shown in Fig. 3(a). Note that the Curie constant, $MT_c=35.7$ K, falls well within the range of published values,[10] as it should of course.

Closer examination of Fig. 1 indicates that the slope γ of the data points is of the order of 1.1, which is rather different from the Curie-Weiss value of 1. This suggests a fit to a power law

$$\epsilon_b=(\epsilon_{b0}+\epsilon_{b1}T)+Mt^{-\gamma} . \tag{6}$$

The estimators are then

$$\epsilon_{b0}=2.87\pm0.04 , \tag{7a}$$

$$\epsilon_{b1}=0.0018\pm0.0002 , \tag{7b}$$

$$M=0.177\pm0.001 , \tag{7c}$$

$$\gamma=1.1045\pm0.0015 , \tag{7d}$$

$$T_c=130.758\pm0.0015 , \tag{7e}$$

where again ϵ_{b1} is measured in units of K^{-1}. The fit is now much better, as indicated by the deviation plot of Fig. 3(b). The change of vertical scale by a factor of 10 between Figs. 3(b) and 3(a) should be noted. The much smaller value of ϵ_{b1} and the value of T_c somewhat closer to the value of T at the peak of ϵ_b are more satisfactory. However, the deviation plot clearly shows a number of zero crossings equal to the number of fit parameters.

It is well documented that logarithmically corrected mean-field behavior can lead to apparent power laws with $\gamma>1$,[38] although the true critical behavior is beyond doubt the logarithmic one.[39] In the case of the uniaxial dipolar system, the LK prediction,[27,6]

$$\chi^{-1}\propto t\,|\,1+g\ln(t_0/t)\,|^{-1/3} , \tag{8}$$

does indeed lead to an effective exponent

$$\gamma_{\rm eff}=\frac{d\ln\chi^{-1}}{d\ln t} , \tag{9}$$

which is 1 in the limit $t\to0$, but which is greater than 1 elsewhere. Equation (8), obtained using Feynman-diagram expansion, has also been confirmed with the renormalization-group approach.[40] Equation (8), which represents a logarithmically accurate solution, has an asymptotic correction of the form[41]

$$\chi^{-1}\propto t\,|\ln t\,|^{-1/3}\left[1+0.3\frac{\ln|\ln t\,|}{|\ln t\,|}\right] . \tag{10}$$

The new term in (10) is zero for $t=e^{-1}$ and diverges at $t=1$. Hence, it is only applicable for small t, where it has a very slow variation. It is thus neglected in the following.

Although the literature contains several discussions of a crossover to mean-field behavior at sufficiently high t,[27,42,43] a suitable functional form for this crossover has *not* been given. In particular, Eq. (8) gives no crossover, as seen by calculating $(\chi t)^3$, which in mean-field theory should be a constant, rather than linear in $\ln t$. The empirical replacement of t by $t/t_0(1+t)$ in the argument of the logarithm, as suggested in Ref. 43, leads, in our case as well as in theirs, to a fitted value $t_0<1$, meaning that the susceptibility has a spurious singularity at $t=t_0/(1-t_0)$, the zero of the ln function. Specifically, a five-parameter fit with a temperature-dependent background as in (6) and a critical part equal to

$$Mt^{-1}\,|\ln t/t_0(1+t)\,|^{1/3} ,$$

leads to $\sigma=8.2\times10^{-4}$ with particularly strong deviations in the region $t\sim t_0/(1-t_0)$. It cannot be considered as an improvement over the power law. In order to avoid this drawback, and to be able to extend our fits to the crossover region, we adopted another empirical expression:

$$\epsilon_b=\epsilon_{b0}+\frac{M}{t}(\ln x)^{1/3} , \tag{11a}$$

where

$$x \equiv \alpha + t_0/t \ . \tag{11b}$$

For $\alpha = t_0$ this coincides with the suggestion of Ref. 43. However, with $\alpha \geq 1$, (11) crosses over to mean field smoothly without passing through a zero of the ln function. For small t, (11) gives

$$\chi^{-1} \propto t \left| \ln t_0/t + \frac{\alpha t}{t_0} \right|^{-1/3} , \tag{12}$$

which asymptotically is closer to Eq. (8) than Eq. (10) is. Hence, Eq. (11) is compatible with the LK theory, and consistent with the neglect of higher-order corrections. It should be noted that the temperature dependence of the background was not included in (11), as the fits were satisfactory with a constant ϵ_{b0}.

The estimators obtained by fitting to Eq. (11) are

$$\epsilon_{b0} = 3.227 \pm 0.006 \ , \tag{13a}$$

$$M = 0.1877 \pm 0.0005 \ , \tag{13b}$$

$$t_0 = 0.274 \pm 0.006 \ , \tag{13c}$$

$$\alpha = 1.69 \pm 0.07 \ , \tag{13d}$$

$$T_c = 130.7745 \pm 0.0005 \tag{13e}$$

where T_c is expressed in units of K. Figure 3(c) demonstrates that the deviations are now governed by statistical errors comparable with our estimated accuracy. The variance σ is three times smaller than that of the power-law fit which used the same number of parameters. It is 40 times smaller than that of the Curie-Weiss fit. The value of T_c is sharply determined and it is now extremely close to the temperature value at which $\epsilon_{b,\max}$ is reached. It is comforting that α is well above 1. The crossover region occurs at rather large[44]

$$t \sim t_0/\alpha = 0.16 = 10^{-0.8} \ .$$

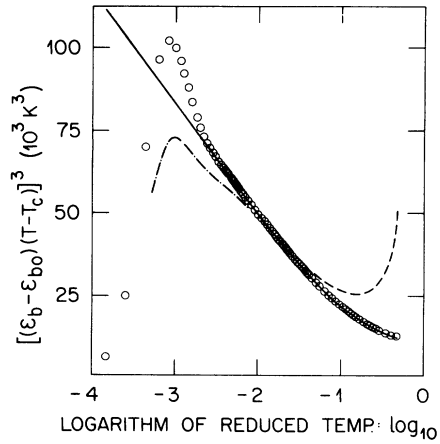

FIG. 4. $[(\epsilon_b - \epsilon_{b0})(T - T_c)]^3$ vs $\log_{10} t$ for the measured data points. Here T_c and ϵ_{b0} have been given their value from Eqs. (13). The dash-dot curve illustrates the modification of the graph obtained when T_c is increased by one part in 10 000. The dashed curve illustrates the effect of a decrease of background by 5%. The solid curve is derived from the fit (13) and illustrates the deviations for $t < t_x$.

To obtain another objective test for the necessity of the log correction, the quantity $[(\epsilon_b - \epsilon_{b0})(T - T_c)]^3$ has been plotted versus log$t$ in Fig. 4. It is obvious from the calculated curves explained in the figure caption that mere adjustment of ϵ_{b0} and T_c is unable to produce a constant value for the quantity plotted, as would be required by mean-field theory. On the contrary, the data points with $t > 10^{-2.6}$ are well explained in terms of logarithmic corrections crossing over to mean field in the region $t \sim 10^{-0.8}$. The uncertainty of the exponent $z = \frac{1}{3}$ in (11a) was investigated in a six-parameter fit, with z as additional parameter. The variance σ is essentially unchanged, whereas the estimators are

$$\epsilon_{b0} = 3.229 \pm 0.011 \ , \tag{14a}$$

$$M = 0.182 \pm 0.017 \ , \tag{14b}$$

$$t_0 = 0.32 \pm 0.14 \ , \tag{14c}$$

$$\alpha = 1.75 \pm 0.20 \ , \tag{14d}$$

$$T_c = 130.7742 \pm 0.0011 \ , \tag{14e}$$

$$z = 0.347 \pm 0.041 \ , \tag{14f}$$

where T_c is expressed in units of K. This fit demonstrates the fine agreement with $z = \frac{1}{3}$, with a modest uncertainty. It also emphasizes the strong correlation between z and the other parameters, as seen from the large increase of their uncertainties, particularly true for the cross-over parameters t_0 and α.

Two features are recognized in Fig. 4 for $t < 10^{-2.6}$: (i) a shoulder, in the region $10^{-3} < t < 10^{-2.6}$, where ϵ_b is anomalously high, and (ii) a strong roundoff which becomes dominant below $t \sim 10^{-3}$. Similarly, extending the $\tilde{\gamma} = -1.5$ line in Fig. 2, one finds a shoulder followed by roundoff, although in this case the shoulder is much enhanced. As will now be explained, considering the successive measurements performed, the shoulder should probably be associated with temperature inhomogeneity and the roundoff with sample quality. After the first sample anneal, and with 50 μm Ø copper leads for contact to the coaxial lines, the shoulder began around $t = 10^{-2.3}$ but the roundoff was strong and interfered with it. After the second anneal, with the same leads, the roundoff was weaker and the shoulder started similarly around $t = 10^{-2.3}$, leading to an increase of its peak value.

A good fit, including the data points in the region $10^{-2.6} < t < 10^{-2.3}$ could nevertheless be obtained by taking a model of inhomogeneous T_c.[45] Specifically, the sample was considered to be a set of parallel capacitors with Gaussian distribution of T_c and of variance $\simeq 50$ mK. Such a model also leads to a much enhanced shoulder in G since, ignoring log corrections, $C \propto t^{-1}$ but $G \propto t^{-\tilde{\gamma}-1} = t^{-2.5}$ for defect theories. As a major source of inhomogeneity can reside in the minute thermal conductivity of the leads, in a third measurement, for which the results are presented above, copper was replaced by brass, which has an order-of-magnitude lower thermal conductivity around 130 K. The measured T_c was then lowered by ~ 0.2 K, consistent with the fact that the colder coax cables had previously been cooling the sample. Also, the beginning of the shoulder was lowered from $t = 10^{-2.3}$ to $t = 10^{-2.6}$, substantiating the above interpretation. Remarkably, the fit parameters (13a)—(13d) are *equal* to those of the second measurement within their accuracy. At this point we felt that there was not much value in trying to improve the temperature homogeneity further as the measurement would be quickly limited by roundoff related to sample quality. In view of the very strong effect that a temperature spread has on G and on tanδ, it is safe to fit ϵ_b down to the point where tanδ starts deviating appreciably from its $t^{-1.5}$ asymptotic behavior (point x) as we have done.

In conclusion, it should be noted that every step we have taken to improve the results (annealing, fringe-field correction, change of leads) has not changed the main qualitative observation that there is a region which can only be well accounted for by log corrections. This makes us strongly confident that the LK behavior is an intrinsic property of TSCC.

IV. DISCUSSION

The measurement of ϵ_b gives quantitative information about the critical behavior of the Landau coefficient A, and demonstrates the great importance of uniaxial dipolar interactions in TSCC. Other measurements ought to be reevaluated in this new light. The present section explores some of the most immediate and important consequences of our result.

The critical part of the dielectric constant below T_c immediately follows from Eq. (11),[6]

$$\epsilon_{\text{crit}} = \frac{1}{2}\frac{M}{|t|}(\ln x)^{1/3} , \tag{15}$$

where x is still given by (11b) with t replaced by $|t|$. Equation (15) has only asymptotic value, and as one penetrates more deeply into the low-temperature phase, saturation effects are likely to become important. These are related to higher-order Landau coefficients (C, D,...) which lead to $P^2 < |A|/B$, where $B \propto 1/\ln x$, and P is the polarization.[6] The same saturation effects give $\epsilon_b < \epsilon_{\text{crit}}$, where ϵ_{crit} is given by Eq. (15). Nevertheless, one can use (15) together with the parameters (13), to obtain a reasonable upper limit to ω_{LO}, the longitudinal optic frequency, using the LST relation

$$\omega_{\text{LO,max}} \simeq \omega_{\text{TO}} \left[1 + \frac{\epsilon_{\text{crit}}}{n^2}\right]^{1/2} . \tag{16}$$

Here, n is the appropriate refractive index, for which we take a value $n = 1.5$ Using for ω_{TO} the curve obtained by Chen *et al.*,[23] one obtains $\omega_{\text{LO,max}}$ as shown in Fig. 5. The two experimental points are drawn according to the LO-TO splitting given explicitly by Prokhorova *et al.*[19] The agreement is as good as it can be, as one should expect a modest influence of saturation at $T_c - 15$ K, and a strong influence at 77 K. Hence, the ω_{LO} behavior is explained without having to call for another instability.[21] This suggests that the main transition mechanism in TSCC is indeed displacive, contrary to earlier beliefs.

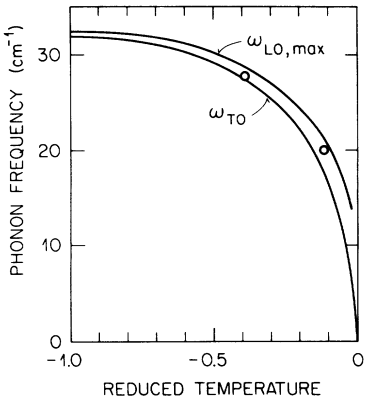

FIG. 5. Soft-mode frequencies: ω_{TO} is taken from Ref. 23, and $\omega_{\text{LO,max}}$ is obtained from Eq. (16). The two data points are for ω_{LO}, using the LO-TO splitting reported in Ref. 19.

A second remark is related to the effective order parameter exponent defined by

$$\beta_{\text{eff}} = \frac{d\ln\langle P\rangle}{d\ln|t|} . \tag{17}$$

In the critical region,

$$\langle P\rangle = \sqrt{-A/B} \propto |t|^{1/2}(\ln x)^{1/3} , \tag{18}$$

which gives

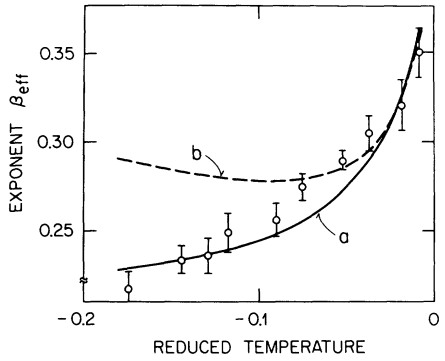

FIG. 6. The effective exponent β_{eff} from Ref. 15. Curve a is obtained from Eq. (19) with $t_0=0.06$ and $\alpha=1.02$. Curve b corresponds to $t_0=0.05$ and $\alpha=1.1$.

$$\beta_{\text{eff}}=\tfrac{1}{2}-\tfrac{1}{3}t_0/[(t_0+\alpha t)\ln x] \simeq \tfrac{1}{2}-\tfrac{1}{3}(\ln x)^{-1} . \quad (19)$$

Clearly, this effective exponent, equal to $\frac{1}{2}$ at T_c, can decrease rapidly as $|t|$ grows and, depending on the values of the nonuniversal parameters t_0 and α, can become as small as $\frac{1}{6}$. If Eq. (19) could be applied in the mean-field region ($\alpha t \gg t_0$), β_{eff} would of course cross over to the mean-field value $\frac{1}{2}$. In fact, here also one should expect saturation which reduces the value of β_{eff}. A comparison of these ideas with the EPR values of[15] β_{eff} is illustrated in Fig. 6. The curves drawn emphasize the great sensitivity of Eq. (19) to the exact values of α and t_0. As these parameters do not necessarily have the same value above and below T_c, and as saturation effects would involve the prefactors of the Landau coefficients B, C, etc., no real fit has been attempted. However, it is quite clear that values of α and t_0 leading to curves between a and b in Fig. 6, together with some modest saturation component, would be able to explain the data perfectly.

A short remark has to do with other measurements of the polarization. Direct measurements usually require a large applied field and could be further complicated by domains. The effect of the applied field should be accounted for carefully.[46,5] Indirect measurements of P, such as refractive index ones,[14] should consider the effect of fluctuations leading to $\langle P^2\rangle \neq \langle P\rangle^2$.

In conclusion, inescapable evidence for log corrections in TSCC has been obtained, in agreement with a recent brief report on the specific heat.[26] This observation is also in qualitative accord with many other published results. The fact is all the more important since results on TGS, for which log corrections had been reported over a narrow temperature range, have been seriously challenged recently.[28,47] It might thus turn out that TSCC is the best current example of uniaxial dipolar behavior in a ferroelectric.

ACKNOWLEDGMENTS

It is a pleasure to thank Professor J. F. Scott for pointing out some current difficulties with TSCC, and for making the crystal of Professor W. Windsch available to us. Thanks are expressed to Dr. R. H. Swendsen and Professor K. A. Müller for helpful remarks in the course of the work. The authors have also benefited from the technical help of Mr. H. Weibel and Mr. P. Bayer, as well as from the use of Dr. U. T. Höchli's equipment. One of us (E.S.) is grateful to Professor K. Fossheim and to IBM Norway for the encouragement and support that made his stay at the IBM Zurich Laboratory possible. One of us (E.C.) is indebted to Professor J. Lajzerowicz for a conversation that led to Ref. 44.

APPENDIX: FRINGING-FIELD CORRECTIONS

We make the approximation of an infinite straight edge (Fig. 7). The solution of the corresponding Laplace equation in vacuum is a standard application of conformal mapping.[48] The additional capacitance due to the charges on the *inside* faces of the plates is given by

$$\Delta C_i=\frac{\Delta Q_i}{V}=\frac{\epsilon_0}{2\pi}L , \quad (A1)$$

where V is the voltage between the plates, ΔQ_i the additional charges given by

$$\Delta Q_i=\int_{-\infty}^{0}\epsilon_0\left[E_y-\frac{V}{d}\right]dx , \quad (A2)$$

and L is the length perpendicular to the xy plane, which in our case is taken to be the perimeter of the sample. The capacitance produced by charges on the *outside* faces of the plate diverges logarithmically with the plate extension in the $-x$ direction.

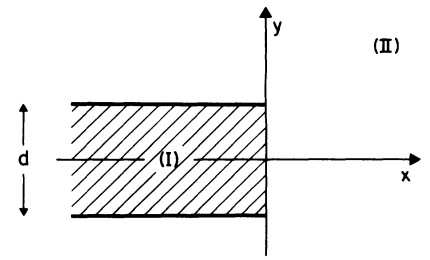

FIG. 7. Edge of a condensor with plates at ($y=\pm d/2$, $-\infty<x<0$). Region I is filled with a dielectric.

This contribution to the background is approximated by Kirchoff's formula[49]

$$\Delta C_0 = \frac{\epsilon_0 L}{2\pi}\left[\ln\frac{16\sqrt{\pi}S}{d} - 1\right], \tag{A3}$$

S being the plate area.

Now, assume that the plates are filled with a dielectric whose dielectric-constant tensor has a principal direction along y, of value ϵ_y. The boundary at $x=0$, $-d/2<y<d/2$, being free of mobile charges, both E_y and D_x are continuous across that boundary. Laplace's equation in both regions I and II can be written

$$\frac{\partial^2 D_x}{\partial \xi^2} + \frac{\partial^2 E_y}{\partial y^2} = 0, \tag{A4}$$

where

$$x = \sqrt{\epsilon_y}\,\xi, \quad \text{in I}, \tag{A5a}$$

and

$$x = \xi, \quad \text{in II}. \tag{A5b}$$

Hence, D_x, E_y satisfy the same equation as that of the vacuum problem, the only difference being a scale compression given by (A5a). Instead of (A2) one has

$$\Delta Q_i = \int_{-\infty}^{0} \epsilon_0 \epsilon_y \left[E_y - \frac{V}{d}\right] dx = \sqrt{\epsilon_y}\int_{-\infty}^{0} \epsilon_0 \left[E_y - \frac{V}{d}\right] d\xi . \tag{A6}$$

Hence, (A1) is now replaced by

$$\Delta C_i = \frac{\epsilon_0}{2\pi}\sqrt{\epsilon_y} L , \tag{A7}$$

while (A3) is unchanged since there is no scale compression in region II. Finally, the measured capacitance C_M is given by

$$C_M = \epsilon_0 \epsilon_y \frac{S}{d} + \frac{\epsilon_0}{2\pi}\sqrt{\epsilon_y} L + \frac{\epsilon_0 L}{2\pi}\left[\ln\frac{16\sqrt{\pi S}}{d} - 1\right]. \tag{A8}$$

and ϵ_y is obtained from C_M by solution of the quadratic equation in $\sqrt{\epsilon_y}$.

*On leave from the Department of Physics, University of Trondheim, 7034-NTH Trondheim, Norway.

[1]R. Pepinsky and Y. Makita, Bull. Am. Phys. Soc. Ser. II 7, 241 (1962).

[2]Y. Makita, J. Phys. Soc. Jpn. 20, 2073 (1965).

[3]T. Ashida, S. Bando, and M. Kakudo, Acta Crystallogr. Sect. B 28, 1560 (1972).

[4]For structure of TGS, see K. Itoh and T. Mitsui, Ferroelectrics 5, 235 (1973).

[5]K. Binder, G. Meissner, and H. Mais, Phys. Rev. B 13, 4890 (1976).

[6]For a recent review, see D. Stauffer, Ferroelectrics 18, 199 (1978).

[7]A. Levstik, C. Filipič, and R. Blinc, Solid State Commun. 18, 1231 (1976).

[8]G. Sorge and U. Straube, Phys. Status Solidi A 51, 117 (1979).

[9]S. Fujimoto, N. Yasuda, K. Takagi, P. S. Narayanan, and H. L. Bhat, J. Phys. D 13, L107 (1980).

[10]J. Bornarel and V. H. Schmidt, J. Phys. C 14, 2017 (1981).

[11]S. Fujimoto, N. Yasuda, and K. Takagi, Jpn. J. Appl. Phys. 20, 1449 (1981).

[12]S. Fujimoto, N. Yasuda, and H. Kashiki, J. Phys. D 15, 487 (1982).

[13]For a table, see Ref. 10.

[14]N. R. Ivanov and H. Arndt, Kristallografiya 24, 508 (1979) [Sov. Phys.—Crystallogr. 24, 291 (1979)].

[15]W. Windsch, Ferroelectrics 12, 63 (1976).

[16]S. Franck, A. Kühnel, T. Nattermann, and S. Wendt, Phys. Status Solidi B 77, 631 (1976).

[17]W. Windsch, R. Lippe, and G. Völkel, Solid State Commun. 17, 1375 (1975).

[18]G. Spörl, S. Ullmann, W. Hässler, E. Hegenbarth, and B. Malike, Phys. Status Solidi A 63, K175 (1981).

[19]S. D. Prokhorova, G. A. Smolensky, I. G. Siny, E. G. Kuzminov, V. D. Mikvabia, and H. Arndt, Ferroelectrics 25, 629 (1980).

[20]L. C. Brunel, J. C. Bureau, S. Wartewig, and W. Windsch, Chem. Phys. Lett. 72, 119 (1980).

[21]G. E. Feldkamp, K. Douglas, B. B. Lavrencič, and J. F. Scott, Bull. Am. Phys. Soc. 25, 171 (1980).

[22]G. E. Feldkamp, J. F. Scott, and W. Windsch, Bull. Am. Phys. Soc. 26, 303 (1981).

[23]T. Chen, G. Schaack, and V. Winterfeldt, Ferroelectrics 39, 1131 (1981).

[24]G. E. Feldkamp, J. F. Scott, and W. Windsch, Ferroelectrics 39, 1163 (1981).

[25]A. López-Echarri and M. J. Tello, J. Phys. D 14, 71 (1981).

[26]M. A. Pérez Jubindo, A. López-Echarri, and M. J. Tello, Ferroelectrics 39, 1171 (1981).

[27]A. I. Larkin and D. E. Khmelnitzkii, Zh. Eksp. Teor. Fiz. 56, 2087 (1969) [Sov. Phys.—JETP 29, 1123 (1969)].

[28]B. A. Strukov, S. A. Taraskin, K. A. Minalva, and V. A. Fedorikhin, Ferroelectrics 25, 399 (1980).

[29]G. Ahlers, A. Kornblit, and H. J. Guggenheim, Phys. Rev. Lett. 34, 1227 (1975); R. Frowein and J. Kötzler, Phys. Rev. B 25, 3292 (1982).

[30]The crystal was kindly supplied by Prof. W. Windsch, Karl-Marx University, Leipzig, German Democratic

Republic.

[31]A. Sawada, Y. Makita, and Y. Takagi, J. Phys. Soc. Jpn. 42, 1918 (1977).

[32]See, e.g., E. Courtens, Phys. Rev. Lett. 41, 1171 (1978).

[33]The equipment was kindly made available by Dr. U. T. Höchli.

[34]Of the form $R=\sum a_i T^i$, with T in degrees K, and

$$a_0=-0.143\,362\,15,\quad a_1=4.6715\times10^{-3},$$

$$a_2=-2.8662\times10^{-6},\quad a_3=5.184\times10^{-9},$$

$$a_4=-4.396\times10^{-12},$$

R being normalized to 1 Ω at 273.15 K.

[35]See AIP document PRBMD-27-5660-3 for three pages of Tables. Order by PAPS number and journal reference from American Institute of Physics, Physics Auxiliary Publication Service, 335 E. 45 St., New York, N.Y. 10017. The price is $1.50 for each microfiche, or $5 for a photocopy. Airmail additional. Make check payable to American Institute of Physics. This material appears in the monthly *Current Physics Microform* edition of all journals published by AIP, on the frames following this article.

[36]A. P. Levanyuk, V. V. Osipov, A. S. Sigov, and A. A. Sobyanin, Zh. Eksp. Teor. Fiz. 76, 345 (1979) [Sov. Phys.—JETP 49, 176 (1979)].

[37]D. W. Marquardt, J. Soc. Ind. Appl. Math. 2, 431 (1963).

[38]See, e.g., M. A. Moore, Phys. Rev. B 1, 2238 (1970).

[39]F. G. Wegner and E. K. Riedel, Phys. Rev. B 7, 248 (1973).

[40]A. Aharony, Phys. Rev. B 8, 3363 (1973).

[41]E. Brézin and J. Zinn-Justin, Phys. Rev. B 13, 251 (1976).

[42]Th. Nattermann, Phys. Status Solidi B 85, 291 (1978).

[43]R. Frowein, J. Kötzler, B. Schaub, and H. G. Schuster, Phys. Rev. B 25, 4905 (1982).

[44]With such a smooth crossover, the exact definition of a crossover temperature t_c is rather arbitrary and sensitive to the crossover function. An order of magnitude estimate of t_c can be obtained by equating the dipolar energy over a correlation range with kT_c [J. Lajzerowicz and J. F. Legrand, Phys. Rev. B 17, 1438 (1978)]. One finds $t_c\sim W_D/kT_c$, where the dipolar energy per site $W_D\sim vP_s^2/4\pi\epsilon_0 Z$ can be estimated from the unit cell volume v, the saturation polarization P_s, and the number of contributing dipoles per cell Z. For TSCC, taking $P_s\sim3\times10^{-3}$ C/m^2, $v=1.6\times10^{-27}$ m^3, and with $Z=4$, one obtains $t_c\sim0.02$. The agreement with the experimental value should be considered satisfactory given the uncertainties and approximations involved, and including the fact that the two crossover criteria are not necessarily identical.

[45]D. J. Bergman, Phys. Rep. 43, 377 (1978). The only model able to fit such a shoulder is model (a) of Fig. 4 (p. 391).

[46]C. Bervillier, J. Phys. Lett. (Paris) 36, L-225 (1975).

[47]K. H. Ehses, H. Meister, and C. Zeyen, Ferroelectrics 20, 287 (1978).

[48]K. J. Binns and P. J. Lawrenson, *Analysis and Computation of Electric and Magnetic Field Problems* (Macmillan, New York, 1963), pp. 163—167.

[49]See, e.g., L. D. Landau, and E. M. Lifshitz, *Electrodynamics of Continuous Media* (Pergamon, Oxford, 1960). See the last problem of Sec. 3 on p. 20.